Journal of Robotics and Control (JRC)
Volume 3, Issue 6, November 2022
ISSN: 2715-5072, DOI: 10.18196/jrc.v3i6.16454

Control of Flexible Manipulator Robots Based on Dynamic Confined Space of Velocities: Dynamic Programming Approach

C. A. Peña Fernández
Department of Electrical Engineering, Federal Institute of Bahia, Salvador - Brazil
Email: cesarfernandez@ifba.edu.br

***Abstract*—Linear Parameter Varying models-based Model Predictive Control (LPV-MPC) has stood out in manipulator robots because it presents well-rejection to dynamic uncertainties in flexible joints. However, it has become too weak when the MPC's optimization problem does not include kinematic constraints-based conditions. This paper uses dynamic confined space of velocities (DCSV) to include these conditions as a recursive polytopic constraint, guaranteeing optimal dependency on a simplex scheduling parameter. To this end, the local frame's velocities and torque/force preload of joints (related to violation of kinematic constraints) are associated with different time scale dynamics such that DCSV correlates them as a polytope. So, a classical LPV-MPC will be updated using a dynamic programming approach according to the DCSV-based polytope. As a result, one lemma about DCSV-based recursive polytope and a five-step procedure for two decoupled close-loop schemes with different time scales compose the LPV-MPC proposed method. Numerical validation shows that even for relevant flexibility situations, trajectory tracking performance is improved by tuning finite horizons and optimization problem constraints regarding DCSV's behavior.**

***Keywords*—Model Predictive Control; Flexibility; Manipulators; Dynamic confined space of velocities; Dynamic programming.**

I. INTRODUCTION

Flexibility in manipulator robots is commonly related to joint motions when bearings and teeth in the gears are worn out, allowing then the violation of the kinematic constraints [1], [2], [2]–[6]. Usually, these motions are modeled as torsional springs with low stiffness, so dynamic models require two time-scales, one for the generalized velocities, usually known as slow variables, and another to represent the violation of the kinematic constraints, usually known as fast variables on singular perturbation approaches [7]–[11].

Mathematically, when kinematic constraints are satisfied for any trajectory in $\mathcal{C}$-space, motions required in the joint space do not need more degrees of freedom. In that context, generalized velocities are a linear combination of vector fields represented by the columns of Jacobian, also known as 1-form distributions. Assuming rigid motions, only the orthogonal complement of Jacobian, also known as 1-form co-distribution, is responsible for the evolution of the kinematic constraints. Nevertheless, with flexibility, generalized velocities depend on both distribution and co-distribution; and kinematic constraints are defined by a symmetric operator acting on the fast variables [12], [13]. Considering this operator is necessary to avoid low manipulability in any control scheme [12], [14]–[16]. Although a good calculus of the Jacobian implies a coherent manipulability for trajectories in $\mathcal{C}$-space, even using a rigid version of the system, the lack of fast variables will induce small transversal and longitudinal motions in the joint space that violate the kinematic constraints.

However, some researchers still assume rigid bodies in the topology of the kinematic configuration and overall dynamic due to the difficulty of controlling joints with small disturbance motions and not because rigidity is technically attractive [7]–[9], [17]–[23]. From that viewpoint, these approaches become rather impracticable in avoiding accidental collisions for tracking tasks and weak tolerance ranges for effort controllers [24]–[26]. In recent years, linearizing control methods have been used to mitigate flexibility effects in trajectory tracking tasks or disturbance (small) motions in the joint space. However, it is well-known that linearization methods are more efficient for approaches based on only one time scale, one fact that needs improvement for two different nature dynamics or singular perturbations-based frameworks [27]–[35]. Although the same problem is partially solved by using optimal programming methods on robust control frameworks or adaptive outer loops, the controller's performance of these approaches gets compromised when the end-effector's velocity increases [27], [29], [30], [36], [37], [37]–[42].

In contrast, integrator backstepping control, supported by sliding manifolds and LQR's methods, consider flexibility as a $\mathcal{L}_2$ disturbance, highlighting that LQR offers better rejection to disturbances, low oscillations, and avoids the chattering phenomenon [8], [33], [42], [43], [43]–[49]. Nevertheless, LQR

The author would like to thank Federal Institute of Bahia (IFBA) and Technological Innovation Center (PIS/IFBA), for the research grant and financial support subject to Announcement n.01/2021-PIS/IFBA and Research Procedure SEI n.23279.005450/2022-48.

needs to offer a suitable rise time and setting time for two timescales, specifically for velocity changing, where relevant flexibility situations cause motion inaccuracy. Therefore, there must be careful with fast variables whose transients with small time responses are undetectable for most known observers and enough to violate the kinematic constraints.

Model predictive control (MPC) has also become a suitable control strategy for handling constrained manipulator robots with input constraints that aim for reasonable behavior forecasts [50]–[54]. However, although MPC performs better than LQR due to its moving time horizon window, in robotic systems, its numeric complexity is increased when two time-scales and parameter varying related to links' guidance are considered [6], [38], [55]. Currently, some techniques suggest a lower computational effort using polytopic representations of the input/output constraints on dynamic programming (DP) methods for linear parameter varying (LPV) [52], [55], [56]. But, although DP's methods reduce the computational cost, this approach is poor for velocity changing.

In [14], [15], Dynamic Confined Space of Velocities (DCSV) was introduced to measure the interrelation between the small transversal and longitudinal motions in joint space and the local velocity of the mobile system. Three components structure the DCSV:

1. Inverse of the norm of the longitudinal violator components of the kinematic constraints;
2. inverse of the norm of the transversal violator components of the kinematic constraints; and
3. norm of the local frame's velocity related to generalized velocities.

In this approach, a set of points with random behavior represents the evolution of the three above components. If these points remain inner to space defined by the DCSV, it is possible to guarantee satisfactory performance of the kinematic constraints [14], [15]. Considering the DCSV from a control viewpoint, recent works show concern about the small violating motions in the joint space but ignore the low manipulability [57]–[62].

The research contribution of this paper is a hybrid LPV-MPC scheme that reduces the impact of flexibility in manipulator robots according to conditions imposed by DCSV and the kinematic constraints. To this end, the classical computed torque technique is applied to linearize the system, being an outer loop that sets static state feedback for slow variables and an inner loop based on the auxiliary control law defined by [14]. Nevertheless, this inner loop will be adapted to a polytopic representation of the DCSV, aiming to compute explicit solutions to the constrained finite-time optimal problem using a DP-based method. This method will include DCSV's parameters in the cost function, and all time-varying parameters will be assumed as accessible online. Finally, instead of solving a constrained finite-time optimal control problem at each sampling, the optimal inputs are precalculated and stored in a lookup table at the same time that suitable velocities at the end-effector of the manipulator robot are assigned.

This paper is organized as follows: Section II presents a generic theoretical framework about robots with two time-scales when linearized by classical CT technique. Sections III and IV detail the formulation of the LPV approach subject to a DCSV-based recursive polytope and a constrained finite-time optimal problem based on the DP technique. Section V presents results on the UR5 robot using CoppeliaSim (V-REP) and free framework YALMIP. Finally, Section VI will make the close remarks.

II. BACKGROUND

Let us consider a n-joint manipulator robot whose configuration $\mathcal{C}$-space can be fully described by the vector of generalized coordinates $q = [q_1\, q_2\, \ldots\, q_n]^T \in D_q \subset \mathbb{R}^n$ where q_j, for $j = 1, \ldots, n$, represents the angle or displacement of the j-th joint. Furthermore, let us consider the following statements:

i. There are k holonomic/nonholonomic velocity constraints represented by $\mathcal{A}(q) \in \mathbb{R}^{n\times k}$ such that $\mathcal{A}^T(q)\dot{q} = 0$. In this way, the linear sensitivity of the end-effector twist $[\mathcal{V}_b] \in se(3)$[1] to the joint velocity $\dot{q}$ can be expressed as $\dot{q} = S_b(q)\mathcal{V}_b$, where $S_b(q) \in \mathbb{R}^{n\times 6}$ is the body Jacobian matrix.

ii. By considering flexible joints, $\mathcal{A}^T(q)\dot{q} \neq 0$ and $\dot{q} \notin \text{cols}(S(q))$. Thus, $\dot{q} = S_b(q)\mathcal{V}_b + \mathcal{A}(q)\varepsilon\mu$, where $\mu \in \mathbb{R}^k$ is a vector associated with the violation of the kinematic constraints and $\varepsilon > 0$ is a scale factor that represents the flexibility [14], [15]. Moreover, since $\mathcal{A}(q)S_b^T(q) = 0$ then $\mathcal{A}^T(q)\dot{q} = \mathcal{A}^T(q)\mathcal{A}(q)\varepsilon\mu$.

iii. The end-effector trajectory is indicated by $(X, \mathcal{V}_b)$, where $X \in SE(3)$ is the current configuration on $\mathcal{C}$-space such that $[\mathcal{V}_b] = X^{-1}\dot{X}$.

iv. Since the pseudo-inverse $(S_b^T S_b)^{-1}S_b^T$ provides the optimal twist $\mathcal{V}_b^*$ when $\dot{q} \notin \text{cols}(S(q))$ then $S_b(q)\mathcal{V}_b^*$ corresponds to the projection of $\dot{q}$ on the spanned space by the columns of $S_b(q)$. So, let $S_p = S_b(S_b^T S_b)^{-1}S_b^T$ be that projection. Knowing that $\mathcal{A}(q)S_b^T(q) = 0$ and $(I_n - S_p)S_p = 0$, the kinematic constraints associated to the configuration X and end-effector can be represented by

$$\mathcal{A}(q) = (I_n - S_b(S_b^T S_b)^{-1}S_b^T)S_b(S_b^T S_b)^{-1} \in \mathbb{R}^{n\times 6}.$$

A generic static state-feedback control for this system is widely defined by

$$\tau = B_\tau^{-1}(q)M(q)S_b(q)\eta + h(q, \dot{q}), \tag{1}$$

[1] $\mathcal{V}_b \in \mathbb{R}^6$ and $se(3)$ is a Lie algebra of the special euclidean group related to rigid-body motions $SE(3)$.

where $B_\tau(q) \in \mathbb{R}^{n\times n}$ is a full-rank matrix, $M(q) \in \mathbb{R}^{n\times n}$ is a symmetric positive-definite mass matrix, $h(q,\dot{q}) \in \mathbb{R}^n$ contains forces that lump together centripetal, coriolis, gravity and friction terms that depends on q, or $\dot{q}$. The vector $\eta \in \mathbb{R}^6$ is an auxiliary control law that ensures the condition $\dot{\mathcal{V}}_b = \eta$, defined by

$$\eta = \dot{C}_{X^{-1}X_d}u + C_{X^{-1}X_d}\dot{u} + K_p\tilde{X} + K_i\int \tilde{X}dt + K_dC_{X^{-1}X_d}u - K_d\mathcal{V}_b \quad (2)$$

being $X_d \in SE(3)$ the target configuration of the end-effector. The matrices K_p, K_d, $K_i \geq 0$ are real and positive semidefinite matrices, the error configuration $\tilde{X}$ must satisfy $[\tilde{X}] = \log(X^{-1}X_d) \in se(3)$ for all adjoint representations of configuration $X^{-1}X_d$, expressed by

$$C_{X^{-1}X_d} = \begin{bmatrix} R_{X^{-1}\dot{X}_d} & 0 \\ \lfloor p_{X^{-1}\dot{X}_d}\rfloor R_{X^{-1}\dot{X}_d} & R_{X^{-1}\dot{X}_d} \end{bmatrix}$$

for $R_{X^{-1}\dot{X}_d} \in SO(3)$, $[p_{X^{-1}\dot{X}_d}] \in so(3)$. The vector $u \in \mathbb{R}^6$ represents the target twist on task-space.

By using (1) and applying the same method in [14], [15], a well-known formulation for a robot on two time-scales, associated with slow and fast variables, is given by

$$\begin{cases} \dot{x} = Z_0(q)\mathcal{V}_b + [\varepsilon Z_1(q) + Z_2(q)]\,\mu \\ \qquad + Z_3(q)B_\tau^{-1}(q)M(q)S_b(q)\eta + Z_3(q)h(q,\dot{q}), & (3) \\ \varepsilon\dot{\mu} = G_0(q)\mathcal{V}_b + [\varepsilon G_1(q) + G_2(q)]\,\mu \\ \qquad + G_3(q)B_\tau^{-1}(q)M(q)S_b(q)\eta + G_3(q)h(q,\dot{q}). & (4) \end{cases}$$

with $x(0) = x_0$, $\mu(0) = \mu_0$, where $x = [\,q\ \mathcal{V}_b\,]^T \in \mathbb{R}^{6+n}$ is the state vector. In the context of singularly perturbed systems, x and μ are associated with slow and fast variables, respectively. The matrices Z_i, G_i (for i=0,1,2,3) have suitable dimension and considered a split representation of the vector fields $Z(x,\mu,\varepsilon,t) = [Z_q(x,\mu,\varepsilon,t)\ Z_{\mathcal{V}_b}(x,\mu,\varepsilon,t)]^T \in \mathbb{R}^{6+n}$ and $G(x,\mu,\varepsilon,t) \in \mathbb{R}^k$, all of them continuously differentiable on the parameters $(x,\mu,\varepsilon,t) \in D_x \times D_\mu \times [0,\varepsilon_0] \times [0,t]$ being $D_x = D_q \cup D_{\mathcal{V}_b} \subset \mathbb{R}^{6+n}$ and $D_\mu \subset \mathbb{R}^k$ open and convex sets. The vector $\tau \triangleq \tau(q,\mathcal{V}_b,\mu) \in \mathbb{R}^n$ contains the torques at motors.

III. Parameter varying and recursive polytope DCSV

Generally, for different $\mathcal{C}$-spaces, the varying parameters are associated with any term that includes harmonic functions of q_i or $\dot{q}_i$. Thus, it will be assumed a vector parameter varying depending on q and $\dot{q}$ defined by $\theta \triangleq \theta(q,\dot{q}) \in \mathbb{R}^{n_\theta}$ such that the system (3)-(4) can be rewritten as

$$\begin{cases} \dot{x} = A_{11}(\theta)x + A_{12}(\theta)\varepsilon\mu + B_x(\theta)\eta + E_1(\theta) & (5) \\ \varepsilon\dot{\mu} = A_{21}(\theta)x + A_{22}(\theta)\varepsilon\mu + B_\mu(\theta)\eta + E_2(\theta), & (6) \end{cases}$$

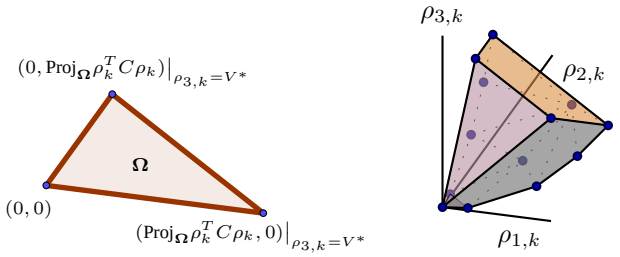

(a) (b)

Fig. 1. (a) Vertices of the recursive polytope $\mathbf{\Omega}$ according to first integral in (13) when $\rho_{3,k} = V^*$, and (b) representation in $\mathbb{R}^3$ of the DCSV, where red faces are associated with planes $\rho_{3,k} = \gamma_{11}\rho_{1,k} + \gamma_{12}\rho_{2,k}$, $\rho_{3,k} = \gamma_{21}\rho_{1,k} + \gamma_{22}\rho_{2,k}$, the yellow face represents the cutting at plane $\rho_{3,k} = V^*$ while the gray faces are associated with first integral (13).

where $A_{11}(\theta) \triangleq [\,0_{n\times n}\ \ Z_0(q)\,]$ is associated with Jacobian matrix between the space of the actuators and the end-effector's twist, and $A_{22}(\theta) \triangleq G_1(q) + \varepsilon^{-1}G_2(q)$ has a strong relationship with the kinematic constraints violation. The matrices $A_{12}(\theta) \triangleq Z_1(q) + \varepsilon^{-1}Z_2(q)$ and $A_{21}(\theta) \triangleq [\,0_{n\times n}\ \ G_0(q)\,]$ are directly responsible by coupling slow and fast variables [63]–[65]. The matrices $B_x(\theta) \triangleq Z_3(q)\Delta(q)$ and $B_\mu(\theta) \triangleq G_3(q)\Delta(q)$, with $\Delta(q) \triangleq B_\tau^{-1}(q)M(q)S_b(q)$, are input matrices.

Since $h(q,\dot{q})$ can be associated with unknown dynamics, acceptable control performance of (1) depends on efficient computing of $h(q,\dot{q})$. Although algorithms based on the inverse dynamic method[2], as well as corrective methods for systems with fast and slow dynamics[3], have been widely used to solve this problem, the work reported here, likewise in [55], considers that $E_1(\theta) \triangleq Z_3(q)h(q,\dot{q})$ and $E_2(\theta) \triangleq G_3(q)h(q,\dot{q})$ admit a polytopic representation.

Let us consider a discrete-time linear parameter-varying system associated with the system (5)-(6) by using a suitable transformation. In this way, it will denoted $a_{i,k}$ as the *i*-th part of the vector a and $a_{k+v|k}$ will denote the predicted state a at the time instant $k+v$, where the prediction will be calculated at the sampling instant k.

Without loss of generality, by using the T. Kato's method [66], like in [55], the system (5)-(6) can be decoupled in two time-scales, as follows:

$$z_{i,k+1} = A_i(\theta_k)z_{i,k} + B_i(\theta_k)\eta_k + E_i(\theta_k)v_k, \quad i = 1,2 \quad (7)$$

where

i. there are n_θ elements in q varying along time that will be considered as the scheduling parameter vector $\theta_k = [\theta_k^{[1]} \dots \theta_k^{[n_\theta]}]^T$. This parameter is measured online such that its future values are barycentric coordinates of a

[2]Euler-lagrange approach by using forward and backward iterations.
[3]Poincaré-Lindstedt technique, neural networks, and backstepping.

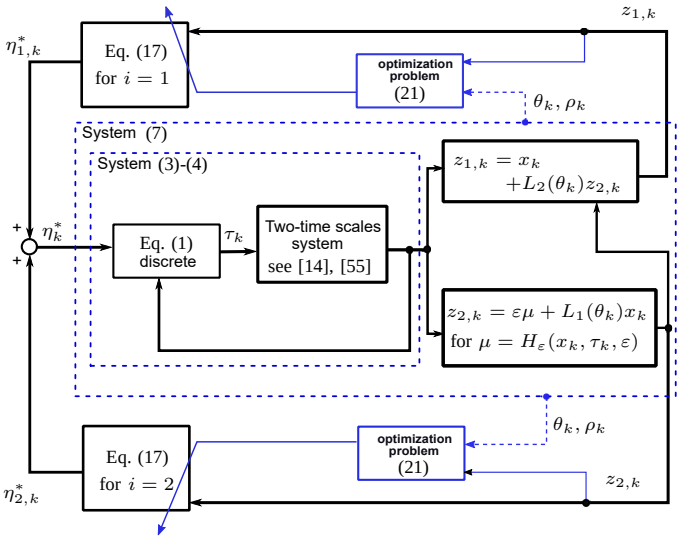

Fig. 2. Control scheme based on an explicit parameter-dependent control law (16) and recursive polytope $\mathbf{\Omega}$. The coordinate transformation at item (*viii*) allows to configure the classical approach based on (1) as the decoupled system (7). By including DCSV as a constraint into the optimal problem (17), the final step **P5** in Algorithm 1 of the MPC approach will guarantee a suitable outer-loop according to the finite horizon N and Pólya degree N_p.

standard n_θ-simplex Θ, i.e.,

$$\theta_k \in \mathbf{\Theta} \triangleq \{\theta_k \in \mathbb{R}^{n_\theta}_+ \mid \sum_{j=1}^{n_\theta} \theta_k^{[j]} = 1\} \subset D_q;$$

ii. $\eta_k \in \mathbb{R}^n$ is the new discrete input vector and $z_k = [z_{1,k}\ z_{2,k}]^T \in \mathbb{R}^{6+n+k}$ is the new discrete state vector, being $z_{1,k}$ associated with slow variables and $z_{2,k}$ associated with fast variables;

iii. $\mathbb{Z}$ and $\mathbb{U}$ are polytopes including the origin in its interior, defined by

$$\mathbb{Z} \triangleq \left\{ z_k \in \mathbb{R}^{6+n+k} | P_z z_k \leq b_z \right\}, \tag{8}$$

$$\mathbb{U} \triangleq \left\{ \eta_k \in \mathbb{R}^6 | P_\eta \eta_k \leq b_\eta \right\}, \tag{9}$$

where P_z, P_η are real matrices of suitable dimensions and b_1, b_2 are known vectors;

iv. there is an invariant manifold $\mu = H(x, \tau(x, \varepsilon), \varepsilon)$ such that $z_{1,k} = x_k + L_2(\theta_k)z_{2,k}$ and $z_{2,k} = \varepsilon\mu + L_1(\theta_k)x_k$, where $L_1(\theta_k) \in \mathbb{R}^{k\times n}$ and $L_2(\theta_k) \in \mathbb{R}^{n\times k}$ satisfy the T. Kato's conditions [66], also used in [55];

v. $A_i(\theta_k)$: $\mathbb{R}^{n_\theta} \to \mathbb{R}^{(6+n+k)\times(6+n+k)}$ is the discrete version of the state matrix, and $B_i(\theta_k)$: $\mathbb{R}^{n_\theta} \to \mathbb{R}^{(6+n+k)\times n}$ is the discrete version of the input matrix; both considered as parameter-varying matrices in the polytopes

$$A_i(\theta_k) = \sum_{j=1}^{n_\theta} A_i^{[j]}\theta_k^{[j]}, \quad B_i(\theta_k) = \sum_{j=1}^{n_\theta} B_i^{[j]}\theta_k^{[j]},$$

where $A_i^{[j]}, B_i^{[j]}$ are j-th vertices.

vi. $E_i(\theta_k) : \mathbb{R}^{n_\theta} \to \mathbb{R}^{(6+n+k)\times n_\upsilon}$ can be associated to an unknown dynamic whose behavior can be modeled like an exogenous disturbance, only bounds on it are known, i.e., $\exists\, \upsilon \in \mathcal{U}$ where $\mathcal{U} \subset \mathbb{R}^{n_\upsilon}$ is a polytope containing the origin and defined by $\mathcal{U} = \{\upsilon : L'\upsilon \leq l\}$, for l and L' known [55].

Although (7) represents a matrix-decoupled model, the parameter simplex Θ continues being the same for all matrices, which is a common assumption in the framework of systems with parameter varying (e.g., [52], [56]). For the problem control makes sense, it will be assumed that the two time-scales dynamic defined by (7) is controllable and observable for all $\theta_k \in \Theta$.

In [14], [15] was shown that $\|z_{2,k}\|$ (related to the fast dynamics μ) and variations of slipping/skidding (associated with longitudinal/transversal small motions in flexible wheels) converge simultaneously to a small neighborhood of the origin. In manipulator roots, torsional motions can represent flexibility; each joint can be equivalent to a linear torsional spring [17], [28], [29], [57], [67], [68]. Nevertheless, synthesizing a control law becomes more difficult with this approach since the end-effector's twist is significantly affected by the slipping associated with preload frictional forces and torques at each joint. Both friction components usually are non-accessible but compose the instrumental meaning of $z_{2,k}$ and therefore, the polytope (8) will be decomposed into two polytopes:

$$\mathbb{Z}_1 \triangleq \left\{ z_{1,k} \in \mathbb{R}^{6+n} | \, P_{z_1} z_{1,k} \leq b_{z,1} \right\}, \text{ and} \tag{10}$$

$$\mathbb{Z}_2 \triangleq \left\{ z_{2,k} \in \mathbb{R}^k | \, P_t z_{2,\tau,k} + P_f z_{2,F,k} \leq b_{z,2} \right\}, \tag{11}$$

where $P_z = [P_{z_1}\ P_t\ P_f]$, for $k = t + f$; $z_{2,\tau,k}$ is associated with the friction torque preload, $z_{2,F,k}$ is associated with the friction force preload and $b_{z,1}, b_{z,2}$ are known vectors.

A. DCSV-based recursive polytope

By using the same notation proposed in [14], [15], the instrumental meaning of $z_{2,k}$ can be used to build a dynamic space known as DCSV as shown in Fig. 1(b), defined by two planes at the first octant ($\rho_{1,k} = 0,\ \rho_{2,k} = 0$) such that

$$\gamma_{11}\rho_{1,k} + \gamma_{12}\rho_{2,k} \leq \rho_{3,k} \leq \gamma_{21}\rho_{1,k} + \gamma_{22}\rho_{2,k}, \tag{12}$$

where $\rho_{1,k} \triangleq \|z_{2,F,k+1}\|^{-1}$, $\rho_{2,k} \triangleq \|z_{2,\tau,k+1}\|^{-1}$ and $\rho_{3,k} \triangleq \|\mathcal{V}_{b,k}\|$, being $\gamma_{11}, \gamma_{12}, \gamma_{21}, \gamma_{22} > 0$ known constants. As indicated in [15], $\gamma_{11}, \gamma_{12}, \gamma_{21}$ and γ_{22} have a direct correspondence with the bounds of the control action, traction force, lateral and longitudinal limits associated with the vector fields ρ_1 and ρ_2, and the maximum value of local frame acceleration. However, according to [14], there is an upper bound $V^* > 0$ such that $\rho_{3,k} \leq V^*$ guarantees asymptotic stability for suitable values of $\varepsilon \leq \varepsilon^*$, where ε^* is formulated by Thikonov's Theorem [14].

Until here, DCSV can be considered partially a polyhedron in $\mathbb{R}^3$, but defining a subset $\mathbf{\Omega} \subseteq \mathbb{R}^2$ such that $\rho_k =$

$[\rho_{1,k}, \rho_{2,k}]^T \in \mathbf{\Omega}$, the constraint $\rho_{3,k} \leq V^*$ can be used to project the DCSV on $\mathbf{\Omega}$ by means a *first integral* $\rho_{3,k}(\rho_k)$:

$$\rho_{3,k}(\rho_k) = \rho_k^T C \rho_k \leq V^*, \tag{13}$$

where $C = \text{diag}(a, b)$, for $a, b > 0$. Thus, even for situations with $a, b >> 0$ the DCSV becomes a bounded space and $\mathbf{\Omega}$ becomes a polytope, see Fig. 1(a).

Lemma 1 (Recursive polytope $\mathbf{\Omega}$)**.** For a n-joint robot based on control law (1) whose decoupled form is defined by (7), if (12) and (13) are satisfied then there exists $p > 1$ and $c = \gamma_{12} - \gamma_{22}$ such that

$$\mathbf{\Omega} = \Bigg\{ \rho_k \in \mathbb{R}^2 \;\mid\; \frac{c}{p} \langle \sigma_{k-1} \left[\begin{smallmatrix} 1 \\ 1 \end{smallmatrix}\right], \rho_k \rangle + \rho_k^T \begin{bmatrix} a & c\frac{1-p}{2p} \\ c\frac{1-p}{2p} & b \end{bmatrix} \rho_k \leq V^* \Bigg\} \tag{14}$$

where $\sigma_k = \|A_2(\theta_k)\|_1 / (\|z_{2,k+1}\|_1 - \|A_2(\theta_k)\|_1 \|z_{2,k}\|_1)$.

Proof. See Appendix. □

While ρ_k satisfies (12), ρ_k remains in $\mathbf{\Omega}$, and the control law acquires better performance to mitigate the flexibility. Based on this last one, the proposal reported here will use this polytope to compute an explicit parameter-dependent control law, as shown in Fig. 2, which guarantees good performance of the polytope $\mathbf{\Omega}$ for each instant k.

Since (1) guarantees $\dot{\mathcal{V}}_b = \eta$, by using the trapezoidal rule for a sample time T_s, the end-effector's twist $\mathcal{V}_b$ can be calculated by $\mathcal{V}_{b,k} = 0.5T_s(2\sum_{j\geq 1}^{k-1} \eta_j + \eta_0 + \eta_k)$, where $\eta_k = 0$ for $k < 0$, for k-th sample. Therefore, the term η_k in (2) can be rewritten as

$$\eta_k = \alpha_{1,k} u_k - \alpha_{2,k} u_{k-1} - d_k \tag{15}$$

where

$$d_k = K_p \tilde{X}_k + T_s K_i \sum_{j\geq 1}^{k-1} \tilde{X}_j + 0.5 T_s K_i (\tilde{X}_0 + \tilde{X}_k) - K_d \mathcal{V}_{b,k}$$
$$\alpha_{1,k} = (2T_s^{-1} + K_d) C_{X^{-1}X_d,k} - T_s^{-1} C_{X^{-1}X_d,k-1}$$
$$\alpha_{2,k} = T_s^{-1} C_{X^{-1}X_d,k}.$$

Nevertheless, according to [14], the control law (15) can be improved by including a weighting function that guarantees better tracking error performance for flexible cases. So, let us consider a discrete version of the weighting function in [14], as follows:

$$h_k = \|z_{2,F,k+1}\| + \|z_{2,\tau,k+1}\| = \rho_{1,k}^{-1}(z_{2,k}, \theta_k) + \rho_{2,k}^{-1}(z_{2,k}, \theta_k),$$

such that (15) can be rewritten as

$$\eta_k' = h_k \eta_k + (h_k - h_{k-1}) \mathcal{V}_{b,k},$$

or even, by substituting the weighting function h_k, the auxiliary law η_k in (15) and $\mathcal{V}_{b,k}$, as

$$\eta_k'(z_k, \theta_k) = f(u_k, z_{1,k}) \sum_{r=1}^{2} \rho_{r,k}^{-1}(z_{2,k}, \theta_k) + g(u_k, z_{1,k}) \sum_{r=1}^{2} \rho_{r,k-1}^{-1}(z_{2,k}, \theta_k), \text{ for} \forall\ \rho_k \in \mathbf{\Omega}, \tag{16}$$

where

$$f(u_k, z_{1,k}) = \frac{1}{2}\Big(3\alpha_{1,k}u_k - 3\alpha_{2,k}u_{k-1} + 2\sum_{p\geq 1}^{k-1} \alpha_{1,p}u_p + 2\sum_{p\geq 1}^{k-1} \alpha_{2,p}u_{p-1} + 3d_k + d_0 + 2\sum_{p\geq 1}^{k-1} d_p\Big),$$
$$g(u_k, z_{1,k}) = \frac{1}{2}\Big(\alpha_{2,k}u_{k-1} - \alpha_{1,k}u_k - 2\sum_{p\geq 1}^{k-1} \alpha_{1,p}u_p - 2\sum_{p\geq 1}^{k-1} \alpha_{2,p}u_{p-1} + d_0 - d_k - 2\sum_{p\geq 1}^{k-1} d_p\Big),$$

being $d_0 = \alpha_{1,0}u_0 - K_d \mathcal{V}_{b,0} + K_p \tilde{X}_0 + T_s K_i \tilde{X}_0$.

For k-th instant, the term d_k is related to solving the forward kinematic problem because the end-effector trajectory $(X, \mathcal{V}_b)$ changes according to the generalized coordinates q (see item (iii)). Hence, since q belongs to slow variables in $z_{1,k}$, the functions f and g will be denoted as $f(u_k, z_{1,k})$ and $g(u_k, z_{1,k})$ to denote the slow part control, i.e., parameter-dependent on $z_{1,k}$.

For this class of systems, it is hoped to find an explicit state-feedback control law dependent on θ_k both slow and fast parts. However, since well-performance of the slow variables decreases when the violation of kinematic constraints becomes notorious, it will be assumed parameter-dependency on θ_k only in fast variables, i.e., $\rho_{r,k}^{-1}(z_{2,k}, \theta_k)$. So, the standard optimization problem for MPC related to η_k' minimizes the cost function that implicitly includes $\rho_{r,k}^{-1}(z_{2,k}, \theta_k)$, guaranteeing an optimal version of (16) and improving the performance of the slow variables.

IV. DP-BASED MPC ON POLYTOPE $\mathbf{\Omega}$

The polynomial dependency of $\rho_{r,k}^{-1}(z_{2,k}, \theta_k)$ on the scheduling parameter has been defined affine on the basis $\mathcal{P}_{r,k} = \{[\rho_{r,k}^{-1}]^1, [\rho_{r,k}^{-1}]^2, \ldots, [\rho_{r,k}^{-1}]^{n_\theta}\}$:

$$\rho_{r,k}^{-1}(z_{2,k}, \theta_k) = \sum_{j=1}^{n_\theta} \theta_k^{[j]} [\rho_{r,k}^{-1}(z_{2,k})]^j$$

where $[\rho_{r,k}^{-1}(z_{2,k})]^j$ is the behavior of $\rho_{r,k}^{-1}$ at j-th vertex of the parameter simplex $\mathbf{\Theta}$. As well-known, on the MPC technique, one cost function based on finite-horizon predictions will be minimized. Over a horizon of length N, these predictions

depend on an unknown sequence of the future scheduling parameters, $\mathcal{T}_k$, a sequence of the control actions, $\mathcal{H}_N$, and a sequence of the DCSV's parameters, $\mathcal{S}_r$, as follows:

$$\begin{aligned}\mathcal{T}_k &= \{\theta_{k+1},\dots,\theta_{k+N-1}\} \in \Theta\times\dots\Theta = \Theta^{N-1},\\ \mathcal{H}_N &= \{\eta'_0,\eta'_1,\dots,\eta'_{N-1}\} \in \mathbb{U}\times\dots\mathbb{U} = \mathbb{U}^{N-1},\\ \mathcal{S}_r &= \{\rho^{-1}_{r,0},\rho^{-1}_{r,1},\dots,\rho^{-1}_{r,N-1}\}_{r=1,2}\\ &= \left\{\sum_{j=1}^{n_\theta}\theta_k^{[j]}[\rho^{-1}_{r,0}(z_{2,k})]^j,\dots,\sum_{j=1}^{n_\theta}\theta_k^{[j]}[\rho^{-1}_{r,N-1}(z_{2,k})]^j\right\}.\end{aligned}$$

Only the first control law η'_0 is applied to decoupled systems in the form (7) whose cost function will be defined by

$$J(\mathcal{T}_k,\mathcal{S}_r;z_k,\theta_k) = \|Pz_{i,k+N}\|_1 + \sum_{j=0}^{N-1}\|Qz_{i,k+j}\|_1 + \|R\eta'_{i,k+j}(z_{i,k+j},\theta_{k+j})\|_1,$$

where P, Q and R are real, full-column rank matrices of appropriate dimensions. The norm $\|\cdot\|_1$ is used to indicate the polyhedral 1-norm, which enables a parametric solution for the optimal problem stated by means DP approach [56].

On the MPC approach, it is assumed that the control law $\eta'_{i,k+j}$ is calculated optimally over the horizon $N-i$ not until $z_{i,k+j}$ and θ_{k+j} are available. After finishing the optimal problem, two optimal control laws will be obtained, $\eta^*_{1,k}$ and $\eta^*_{2,k}$, one for each subsystem in (7). So, the combined optimal control will be defined by

$$\begin{aligned}&\eta^*_{i,k} = \arg\min_{\mathcal{S}_{r,0}}\max_{\theta_{k+1}}\min_{\mathcal{S}_{r,1}}\dots\max_{\theta_{k+N-1}}\min_{\mathcal{S}_{r,N-1}} J(\mathcal{T}_k,\mathcal{S}_r;z_k,\theta_k)\\ &\text{s.t. } \forall j\in\{0,\dots,N-1\};\\ &z_{i,k+j+1} = A_i(\theta_{k+j})z_{i,k+j} + B_i(\theta_{k+j})\eta'_{i,j}(z_{k+j},\theta_{k+j}) + E_i(\theta_{k+j})\upsilon_{k+j};\\ &\eta'_{i,j}(z_{k+j},\theta_{k+j})\in\mathbb{U},\ \forall\mathcal{T}_k\in\Theta^{N-1};\\ &\rho_{k+j}\in\mathbf{\Omega},\ \forall\mathcal{T}_k\in\Theta^{N-1};\\ &z_{i,k+N}\in\mathbb{Z}_{T,i},\ \forall\mathcal{T}_k\in\Theta^{N-1};\\ &z_{i,k+j}\in\mathbb{Z}_i,\ \forall\mathcal{T}_k\in\Theta^{N-1};\\ &\theta_{k+j}\in\Theta,\end{aligned} \tag{17}$$

for $i=1,2$, where $\mathbb{Z}_{T,i}$ represents the polytopic terminal state constraints and

$$\eta'_{i,j}(z_{k+j},\theta_{k+j}) = f(u_j,z_{1,k+j})\sum_{r=1}^{2}\rho^{-1}_{r,k+j}(z_{2,k+j},\theta_{k+j}) + g(u_j,z_{1,k+j})\sum_{r=1}^{2}\rho^{-1}_{r,k+j-1}(z_{2,k+j},\theta_{k+j}).$$

Conventionally, the DP procedure to solve (17) is started at the prediction horizon N, for $i=1,2$, with

$$J^*_N(z_{i,k+N}) = \|Pz_{i,k+N}\|_1.$$

At each iteration, the right side of (7) is used to substitute $z_{i,k+j+1}$ in $J_j(z_{i,k_j})$, for the $k+j$-th instant. As θ_{k+j} is unknown for $j>0$, the proposed DP approach will start from the worst case, which allows solving the following optimization problem by iterating backward (decreasing from $N-1$ to 1):

$$\begin{aligned}&J^*_j(z_{i,k+j},\theta_k) = \|Qz_{i,k+j}\|_1 + \max_{\theta_{k+j}}\min_{\mathcal{S}_{r,j}}\|R\eta'_{i,j}(z_{k+j},\theta_{k+j})\|_1 + J^*_{j+1}(z_{i,k+j+1})\\ &\text{s.t.}\\ &z_{i,k+j+1} = A_i(\theta_{k+j})z_{i,k+j} + B_i(\theta_{k+j})\eta'_{i,j}(z_{k+j},\theta_{k+j}) + E_i(\theta_{k+j})\upsilon_{k+j};\\ &\rho_{k+j}\in\mathbf{\Omega},\ \forall\theta_{k+j}\in\Theta;\\ &\eta'_{i,j}(z_{k+j},\theta_{k+j})\in\mathbb{U},\ \forall\theta_{k+j}\in\Theta;\\ &z_{i,k+j+1}\in\mathbb{Z}_{i,j+1},\ \forall\theta_{k+j}\in\Theta;\\ &z_{i,k+j}\in\mathbb{Z}_i;\\ &\theta_{k+j}\in\Theta,\end{aligned} \tag{18}$$

where $\mathbb{Z}_{i,j+1}$ denotes the polytopic set of successor states for which (18) is feasible at iteration j.

In order to determine the worst-case parameters of (18), an epigraph reformulation in the optimization problem will be applied to transfer the parameter dependence to the constraints, yielding

$$\begin{aligned}&J^*_j(z_{i,k+j}) = \min_{\mathcal{S}_{r,k+j}} w\\ &\text{s.t. } \forall\theta_{k+j}\in\Theta,\\ &\|Qz_{i,k+j}\|_1 + \|R\eta'_{i,k+j}(z_{k+j},\theta_{k+j})\|_1 + J^*_{j+1}(A_i(\theta_{k+j})z_{i,k+j} + B_i(\theta_{k+j})\eta'_{i,k+j}(z_{k+j},\theta_{k+j}) + E_i(\theta_{k+j})\upsilon_{k+j})\le w\\ &\rho_{k+j}\in\mathbf{\Omega};\\ &\eta'_{i,k+j}(z_{k+j},\theta_{k+j})\in\mathbb{U};\\ &z_{i,k+j}\in\mathbb{Z}_i.\end{aligned} \tag{19}$$

According [56], since $B_i(\theta_k)$ is not constant and η'_k is a polynomial parametrized (due to $\rho^{-1}_{r,k}(z_{2,k},\theta_k)$ to be also polynomial parametrized) then the constraint satisfaction of the semi-definite optimization problem (19) can be conservatively ensured over the whole parameter simplex $\mathbf{\Theta}$ by using the Pólya's theorem.

Theorem 1 (Pólya's theorem)**.** If a homogeneus polynomial $p(\theta)$ is positive on the simplex Θ, all the coefficients of

$$p_{N_p}(\theta) = p(\theta)\cdot\left(\sum_{j=1}^{n_\theta}\theta^{[j]}\right)^{N_p}$$

are positive for a sufficiently large Pólya degree N_p.

Proof. See [69]. □

Algorithm 1 Calculating η_k^*

Input: degree d, constraints in (19)

Output: $\eta_k^* = \eta_{1,k}^* + \eta_{2,k}^*$

1: **P1:** Reformulate constraints in (19) as polynomials in θ_k into positivity constraints by using item (ix),

$$w - J_{j+1}^*(A_i(\theta_{k+j})z_{i,k+j} + B_i(\theta_{k+j})\eta'_{i,k+j}(z_{k+j},\theta_{k+j}) + E_i(\theta_{k+j})\upsilon_{k+j}) \geq 0, \quad \forall\, \theta_{k+j}, \in \boldsymbol{\Theta}\, \rho_{k+j} \in \boldsymbol{\Omega}; \tag{20}$$

where d will be its degree.

2: **P2:** Homogenize polynomial obtained before by multiplying single monomials $\sum_{j=1}^{n_\theta} \theta^{[j]}$ until all monomials have the same degree.

3: **P3:** According to [69], let us denote the maximum of scaled coefficients of (20) by $L_{\max}$ and the minimum by $L_{\min}$, if

$$N_p > \frac{d(d-1)}{2}\frac{L_{\max}}{L_{\min}} - d,$$

then (20) multiplied by $(\sum_{j=1}^{n_\theta} \theta^{[j]})^{N_p}$ will have positive coefficients. Let us denote these coefficients as c_{N_p}.

4: **P4:** Replace the constraints by $c_{N_p}(z_{i,k+j}, \mathcal{S}_{r,k+j}, w) \geq 0$;

5: **P5:** Calculate $\eta_k^* = \eta_{1,k}^* + \eta_{2,k}^*$.

6: **return** η_k^*.

Therefore, if the constraints in (19), formulated as homogeneous polynomial, are positive on the simplex $\boldsymbol{\Theta}$ then all coefficients of these constraints multiplied by $(\sum_{j=1}^{n_\theta} \theta^{[j]})^{N_p}$ are positive for a sufficiently large Pólya degree N_p. In this way, an explicit LPV-MPC technique formulated according to DP procedure is defined by five steps, as shown in Algorithm 1.

When $j = 1$, the DP procedure must consider the current parameter θ_k instead of using the worst case. Nevertheless, $J_j^*(z_{i,k+j}, \theta_k)$ in (18) is a bilinear function in $z_{i,k}$ and θ_k, and bilinear constraints are also present in the minimization problem, avoiding a standard multiparametric solution strategy. For this reason, the optimal problem (19) will be based on the uncontrolled sucessor state $\hat{v}_{i,k} = (\sum_{j=1}^{n_\theta} A_i^{[j]}\theta_k^{[j]})z_{i,k}$ and a new epigraph variable s. So,

$$\begin{aligned} J^*(\hat{v}_{i,k}) &= \min_{\mathcal{S}_{r,k}} w + s \\ &\text{s.t. } \forall \theta_k \in \Theta, \\ &\|R\eta'_{i,k}(\hat{v}_{i,k},\theta_{k+1})\|_1 + J_1^*(\hat{v}_{i,k} + B_i(\theta_k)\eta'_{i,k}(\hat{v}_{i,k},\theta_k) \\ &\qquad + E_i(\theta_k)\upsilon_k) \leq w \\ &\epsilon' \sum_{j=1}^{n_\theta} \|Q(\hat{v}_{i,k} + B(\theta_k^{[j]})\eta'_{i,k}(\hat{v}_{i,k},\theta_{k+1}))\|_1 \leq s; \\ &\rho_k \in \boldsymbol{\Omega}; \\ &\eta'_{i,k}(\hat{v}_k,\theta_k) \in \mathbb{U}, \end{aligned} \tag{21}$$

where $0 < \epsilon' << 1$ penalizes the vertex predictions such that the non-uniqueness of the vertex solutions is mitigated.

V. Accessing DCSV-based MPC: results

This section consists of numerical validations based on the manipulator UR5, whose technical specifications and details about matrices in the model (3)-(4) are widely available in the current literature (e.g., [14], [15], [67]). This robot has six revolute joints; therefore, the scheduling parameter θ_k will equal generalized coordinates in q, i.e., $n_\theta = 6 = \dim\{q\}$. For the inner loop based on (1), the parameters K_p, K_i, K_d were set as $10.0, 0.0$ and 18.0, respectively, to guarantee Hurwitz's criterium. The global branch-and-bound based solver in YALMIP was used to compute optimization problems, like (19) and (21). Simulations were executed using the remote API to communicate CoppeliaSim (V-REP) with MATLAB®.

Flexibility was induced by including disturbances in the first joint's motion (associated with $q_1 \triangleq \theta_k^{[1]}$) as spring-damper mode controllers; specifically, modifying spring constant and damping coefficient to impose small opposite torsional motions that violate the kinematic constraints of subsequent joints. To this end, two cases will be analyzed based on the spring constant K and damping coefficient C: **CASE 1**, (K, C)=(1×10^{11}, 1×10^{8}) and **CASE 2**, (K, C)=(9.025,6.650).

Fig. 5 shows the evolution of the end-effector trajectory tracking, starting at (**-0.4872, 0.5672, 0.1487**) and ending at (**-0.4872, 0.256, 0.589**), where θ_k courses $\mathcal{C}$-space beginning at $[0\ 0\ 0\ 0\ 0\ 0]$ and finishing at $[0\ 0\ -\frac{\pi}{2}\ \frac{\pi}{6}\ 0\ 0]$. Two strategies were applied, one associated with the classical auxiliary law (2) for CASES 1 and 2 (label: **`aux02`**), and one another associated with the explicit parameter-dependent control law (16) based on polytope $\boldsymbol{\Omega}$, optimization problem (21) and step **P5** in Algorithm 1 (label: **`aux16`**).

The classical approach of (2) is generally used for libraries available in frameworks for robotic systems, as shown in [67], while the approach based on (16) has been partially studied in [55]. Improvements in that approach are just the main focus of this paper.

Fig. 3 shows in six-time stages the behavior of UR5 in CoppeliaSim after applying **`aux02`**.

According to items (ii) and (iv), it was computed, simultaneously with the path tracking, the evolution of the kinematic constraints for both flexibility cases, as shown in Fig. 6. To this end, it was used the ∞-norm as follows:

$$\|\mathcal{A}^T(q)\dot{q}\|_\infty = \varepsilon\|\mathcal{A}^T(q)\mathcal{A}(q)\mu\|_\infty.$$

Note that the vertical scale in Fig. 6 gives a notion about the order of ε.

In Fig. 5 can be noted that by using **`aux16`** with $N = 2$ and $N_p = 2$, the path tracking is better than **`aux02`**. However, the end-effector does not reach the end point because the

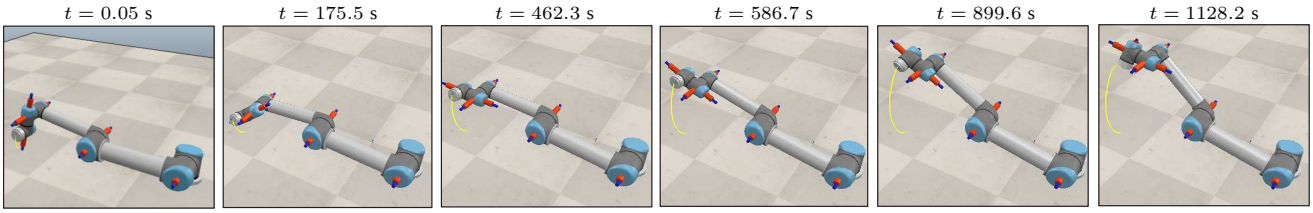

Fig. 3. Evolution of the path tracking for UR5 in CoppeliaSim by using $K_p = 10.0, K_i = 0.0, K_d = 18.0$ in the control law (2). The plotted path corresponds to the CASE 2 and label **aux02** in Fig. 5.

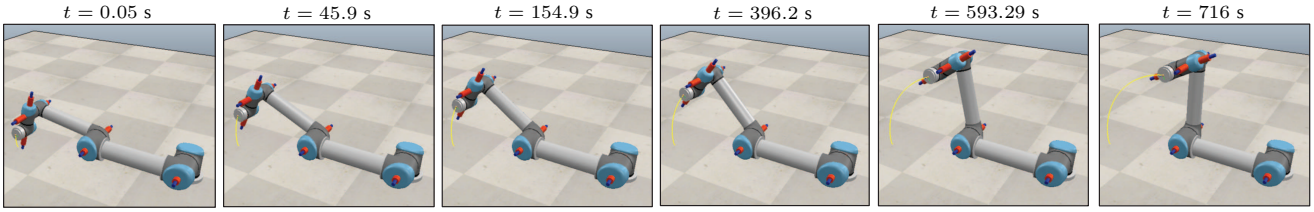

Fig. 4. Evolution of the path tracking for UR5 in CoppeliaSim by using $K_p = 10.0, K_i = 0.0, K_d = 18.0$, $N = 3$ and $N_p = 5$ in the explicit parameter-dependent control law (16) associated with optimal problem (21). The plotted path corresponds to the CASE 1 and label **aux16N** in Fig. 5.

compensation for the additional torsional effect imposed by the first joint is insufficient.

After setting $N = 3$ and $N_p = 5$, the trajectory tracking and the behavior of the kinematic constraints are shown in Fig. 5 (label: **aux16N**) and Fig. 6b, respectively. Note that the tracking was improved, and the scale in Fig. 6b ($\times 10^{-10}$) is lower than noted in Fig. 6a ($\times 10^{-6}$). Hence, according to notation $\varepsilon \|\mathcal{A}^T(q)\mathcal{A}(q)\mu\|_\infty$, it can be possible to infer that ε was changed from order 10^{-6} to order 10^{-10}, i.e., the motion became closer to the rigid conditions, improving the performance of the control law (16). Finally, Fig. 4 shows the path tracking after applying the explicit parameter-dependent control law (16) with $N = 3$ and $N_p = 5$.

VI. Final Remarks

The work reported here proposes an LPV-MPC technique based on the explicit parameter-dependent control law (16), and a recursive polytope $\mathbf{\Omega}$ to include the constraints proposed by the DCSV for flexible manipulator robots. To this end, techniques on system decoupling were applied in Section III, and outputs associated with two time scales were subjected to polytopic representations, specifically slow and fast dynamics. Next, Lemma 1 proposes an equivalent condition to the DCSV such that the weighting function presented in [14] guarantees the suitable performance of the control law (16). In this way, Section IV includes polynomial dependence on θ_k for components of the weighting function and proposes five steps (**P1**-**P5**) aided by a dynamic programming approach that returns an optimal control law η_k^* (see step **P5** in Algorithm 1). Results make sense when the finite horizon N and N_p increase, guaranteeing better path tracking and a significant decrease in flexibility.

Although the method reported here was used only in manipulator robots, the flexibility is also presented in other robotic systems, e.g., wheeled mobile robots and unmanned aerial vehicles. Future works can use the proposed control scheme to reduce the impact of the deformable contact area between different kinds of wheels and the motion's surface, responsible mainly for inducing flexibility to specific traction tasks. In the same way, flexible wings and other parts in unmanned vehicles could also be compensated by using the DCSV, not only as criterium to improve the controller's performance but also as criterium for selecting suitable kinematic configurations.

Appendix

Proof of Lemma 1

By using the 1-norm, note that $h_k = \rho_{1,k}^{-1} + \rho_{2,k}^{-1} = \|z_{2,\tau,k+1}\|_1 + \|z_{2,F,k+1}\|_1 = \|z_{2,k+1}\|_1$, and by applying the Minkowski and Cauchy-Schwarz inequalities in (7) as well as the control law η_k', for $i = 2$, yields

$$\rho_{1,k}^{-1} + \rho_{2,k}^{-1} \leq \|A_2(\theta_k)\|_1 \rho_{1,k-1}^{-1} + \|A_2(\theta_k)\|_1 \rho_{2,k-1}^{-1} + \|B_2(\theta_k)\|_1 \|\eta_k^*\|_1 + \|E_2(\theta_k)\|_1 \|\upsilon_k\|_1,$$

or even, by using a slack function $\delta_k > 0$ such that

$$\rho_{1,k}^{-1} + \rho_{2,k}^{-1} = \|A_2(\theta_k)\|_1 \rho_{1,k-1}^{-1} + \|A_2(\theta_k)\|_1 \rho_{2,k-1}^{-1} + \|B_2(\theta_k)\|_1 \|\eta_k^*\|_1 + \|E_2(\theta_k)\|_1 \|\upsilon_k\|_1 - \delta_k.$$

Moreover, since $E_2(\theta_k)$ is associated with an unknown dynamic, expressed as an exogenous disturbance, both terms

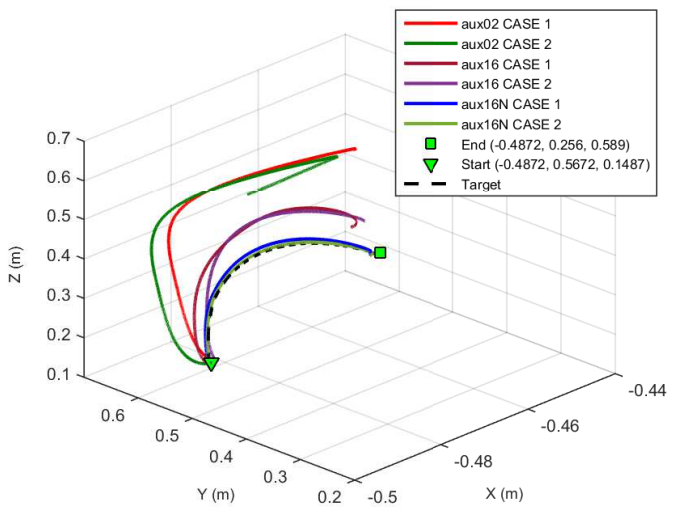

Fig. 5. Trajectory tracking by using the explicit parameter-dependent control law (16) and the classical auxiliary law (2) (**aux02**) for two flexibility cases (CASE 1 and CASE 2 based on spring-damper mode for the fist joint). Law (16) was set according two situations: **aux16**, with $N = N_p = 2$, and **aux16N**, with $N = 3, N_p = 5$

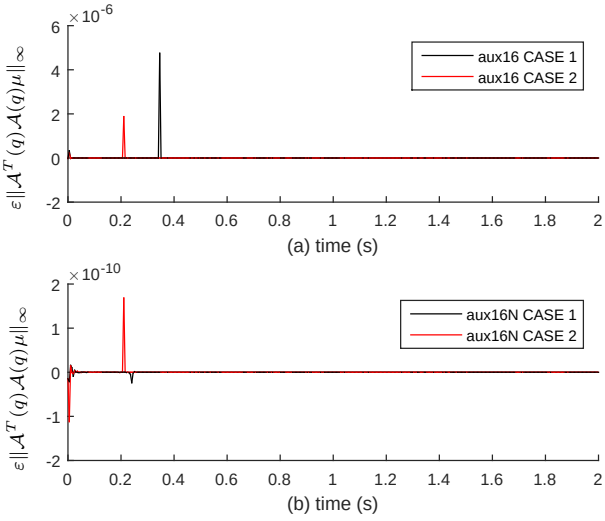

Fig. 6. Evolution of the kinematic constraints (at pfaffian form) according to items (ii) and (iv) such that $\|\mathcal{A}^T(q)\dot{q}\|_\infty = \varepsilon\|\mathcal{A}^T(q)\mathcal{A}(q)\mu\|_\infty$. From (a) and (b), it can be noted that ε is strongly associated with ε's reduction like happens for the control law **aux16N** in Fig.5.

$\|E_2(\theta_k)\|_1\|\upsilon_k\|_1$ and δ_k can be redefined as $\epsilon(\theta_k) = \|E_2(\theta_k)\|_1\|\upsilon_k\|_1 - \delta_k$. Thus,

$$\rho_{1,k}^{-1} + \rho_{2,k}^{-1} = \|A_2(\theta_k)\|_1\rho_{1,k-1}^{-1} + \|A_2(\theta_k)\|_1\rho_{2,k-1}^{-1} + \|B_2(\theta_k)\|_1\|\eta_k^*\|_1 + \epsilon(\theta_k),$$

or, by defining $f_2(\theta_k) = \|B_2(\theta_k)\|_1\|\eta_k^*\|_1 + \epsilon(\theta_k)$, as

$$\rho_{1,k}^{-1} + \rho_{2,k}^{-1} = \|A_2(\theta_k)\|_1\rho_{1,k-1}^{-1} + \|A_2(\theta_k)\|_1\rho_{2,k-1}^{-1} + f_2(\theta_k). \quad (22)$$

Considering $\epsilon^*(\theta_k) = \|A_2(\theta_k)\|_1\rho_{1,k-1}^{-1} - \rho_{2,k}^{-1}$, the inequality (12) can be rewritten as

$$\lambda_1\epsilon^*(\theta_k) + \gamma_{12}f_2(\theta_k) + \frac{\gamma_{11}}{\rho_{1,k-1}}\|A_2(\theta_k)\|_1 + \frac{\gamma_{12}}{\rho_{2,k-1}}\|A_2(\theta_k)\|_1 \leq \frac{\rho_{3,k}}{\rho_{1,k}\rho_{2,k}} \quad (23)$$

$$\lambda_2\epsilon^*(\theta_k) + \gamma_{22}f_2(\theta_k) + \frac{\gamma_{21}}{\rho_{1,k-1}}\|A_2(\theta_k)\|_1 + \frac{\gamma_{22}}{\rho_{2,k-1}}\|A_2(\theta_k)\|_1 \geq \frac{\rho_{3,k}}{\rho_{1,k}\rho_{2,k}}, \quad (24)$$

where $\lambda_1 = \gamma_{12} - \gamma_{11}$ and $\lambda_2 = \gamma_{22} - \gamma_{21}$. By adding (23) and (24) yields

$$\rho_{2,k-1}\rho_{1,k-1}[\lambda_3\epsilon^*(\theta_k) + \lambda_4 f_2(\theta_k)] + \lambda_5\rho_{2,k-1}\|A_2(\theta_k)\|_1 + \lambda_4\rho_{1,k-1}\|A_2(\theta_k)\|_1 \leq 0$$

where $\lambda_3 = \lambda_1 - \lambda_2$, $c_2 = \gamma_{12} - \gamma_{22}$ and $\lambda_5 = \gamma_{11} - \gamma_{21}$, or even,

$$c_1\rho_{2,k}\rho_{2,k-1}\|A_2(\theta_k)\|_1 + c_2\rho_{1,k-1}\rho_{2,k}\|A_2(\theta_k)\|_1 + c_2\rho_{2,k}\rho_{2,k-1}\rho_{1,k-1}f_2(\theta_k) - \lambda_3\rho_{2,k-1}\rho_{1,k-1} \leq 0$$

where $c_1 = \lambda_3 + \lambda_5$. But, it is necessary that at least $c_2\rho_{2,k} \leq \frac{\lambda_3}{pf_2(\theta_k)}$, for $p > 1$, to guarantee the before inequality i.e.,

$$c_1\lambda_3\frac{\|A_2(\theta_k)\|_1}{pc_2f_2(\theta_k)}\rho_{2,k-1} + \lambda_3\frac{\|A_2(\theta_k)\|_1}{pf_2(\theta_k)}\rho_{1,k-1} + \lambda_3\frac{1-p}{p}\rho_{2,k-1}\rho_{1,k-1} \leq 0. \quad (25)$$

According to (13), the inequality $a\rho_{1,k-1}^2 + b\rho_{2,k-1}^2 \leq V^*$ is also satisfied, and by adding this last one with (25) yields

$$c_1\frac{\|A_2(\theta_k)\|_1}{pf_2(\theta_k)}\rho_{2,k-1} + c_2\frac{\|A_2(\theta_k)\|_1}{pf_2(\theta_k)}\rho_{1,k-1} + c_2\frac{1-p}{p}\rho_{2,k-1}\rho_{1,k-1} + a\rho_{1,k-1}^2 + b\rho_{2,k-1}^2 \leq V^*.$$

Since $\rho_{1,k}^{-1} + \rho_{2,k}^{-1} = \|z_{2,\tau,k+1}\|_1 + \|z_{2,F,k+1}\|_1 = \|z_{2,k+1}\|_1$, it can be noted that $f_2(\theta_k) = \|z_{2,k+1}\|_1 - \|A_2(\theta_k)\|_1\|z_{2,k}\|_1$ and $c_1 = c_2 = \gamma_{12} - \gamma_{22}$, thus by defining $c = \gamma_{12} - \gamma_{22}$ and by using the vectorial notation $\rho_k = [\rho_{1,k}, \rho_{2,k}]^T$, for $(k-1)$-th sample, the left side can be expressed as

$$\frac{c\|A_2(\theta_k)\|_1}{p(\|z_{2,k+1}\|_1 - \|A_2(\theta_k)\|_1\|z_{2,k}\|_1)}\begin{bmatrix}1\\1\end{bmatrix}\cdot\rho_{k-1} + \rho_{k-1}^T\begin{bmatrix}a & c\frac{1-p}{2p}\\ c\frac{1-p}{2p} & b\end{bmatrix}\rho_{k-1} \leq V^*.$$

This last one ends the proof.

ACKNOWLEDGMENT

The author would like to thank Federal Institute of Bahia (IFBA) and Technological Innovation Center (PIS/IFBA), for

the research grant and financial support subject to Announcement n.01/2021-PIS/IFBA and Research Procedure SEI n.23279.005450/2022-48.

REFERENCES

[1] Z. Chen, J. Li, S. Wang, J. Wang, and L. Ma, "Flexible gait transition for six wheel-legged robot with unstructured terrains," *Robotics and Autonomous Systems*, vol. 150, p. 103989, apr 2022.

[2] P. Balatti, M. Leonori, and A. Ajoudani, "A flexible and collaborative approach to robotic box-filling and item sorting," *Robotics and Autonomous Systems*, vol. 146, p. 103888, dec 2021.

[3] J. Agrawal, W. Chi, S. Chien, G. Rabideau, D. Gaines, and S. Kuhn, "Analyzing the effectiveness of rescheduling and flexible execution methods to address uncertainty in execution duration for a planetary rover," *Robotics and Autonomous Systems*, vol. 140, p. 103758, jun 2021.

[4] L. Cui, H. Wang, and W. Chen, "Trajectory planning of a spatial flexible manipulator for vibration suppression," *Robotics and Autonomous Systems*, vol. 123, p. 103316, jan 2020.

[5] S. Wang, H. Zhou, C. Zhang, L. Ge, W. Li, T. Yuan, W. Zhang, and J. Zhang, "Design, development and evaluation of latex harvesting robot based on flexible toggle," *Robotics and Autonomous Systems*, vol. 147, p. 103906, jan 2022.

[6] M. Faroni, M. Beschi, C. G. L. Bianco, and A. Visioli, "Predictive joint trajectory scaling for manipulators with kinodynamic constraints," *Control Engineering Practice*, vol. 95, p. 104264, feb 2020.

[7] A. Cibicik and O. Egeland, "Kinematics and dynamics of flexible robotic manipulators using dual screws," *IEEE Transactions on Robotics*, vol. 37, no. 1, pp. 206–224, feb 2021.

[8] C. Chen, C. Zhang, T. Hu, H. Ni, and Q. Chen, "Finite-time tracking control for uncertain robotic manipulators using backstepping method and novel extended state observer," *International Journal of Advanced Robotic Systems*, vol. 16, no. 3, p. 172988141984465, may 2019.

[9] W. He, Z. Yan, Y. Sun, Y. Ou, and C. Sun, "Neural-learning-based control for a constrained robotic manipulator with flexible joints," *IEEE Transactions on Neural Networks and Learning Systems*, vol. 29, no. 12, pp. 5993–6003, dec 2018.

[10] H. Gao, W. He, C. Zhou, and C. Sun, "Neural network control of a two-link flexible robotic manipulator using assumed mode method," *IEEE Transactions on Industrial Informatics*, vol. 15, no. 2, pp. 755–765, feb 2019.

[11] D. Shang, X. Li, M. Yin, and F. Li, "Dynamic modeling and control for dual-flexible servo system considering two-dimensional deformation based on neural network compensation," *Mechanism and Machine Theory*, vol. 175, p. 104954, sep 2022.

[12] B. D'Andréa-Novel, G. Campion, and G. Bastin, "Control of wheeled mobile robots not satisfying ideal velocity constraints: A singular perturbation approach," *International Journal of Robust and Nonlinear Control*, vol. 5, no. 4, pp. 243–267, 1995.

[13] R. M. Murray, Z. Li, and S. S. Sastry, *A Mathematical Introduction to Robotic Manipulation*, First ed. CRC Press LLC, 1994.

[14] C. P. Fernández, J. Cerqueira, and A. Lima, "Nonlinear trajectory tracking controller for wheeled mobile robots by using a flexible auxiliary law based on slipping and skidding variations," *Robotics and Autonomous Systems*, vol. 118, pp. 231–250, aug 2019.

[15] C. A. Peña Fernández, J. J. F. Cerqueira, and A. M. N. Lima, "Trajectory control of wheeled mobile robots not satisfying ideal velocity constraints by using slipping and skidding variations: A singular perturbation approach," in *Communications in Computer and Information Science*. Springer Berlin Heidelberg, 2015, pp. 74–95.

[16] ——, "Control of wheeled mobile robots singularly perturbed by using slipping and skidding variations: curvilinear coordinates approach (part i)," in *Proceedings of 11th IFAC Symposium on Robot Control*, 2015.

[17] M. W. Spong, "An historical perspective on the control of robotic manipulators," *Annual Review of Control, Robotics, and Autonomous Systems*, vol. 5, no. 1, pp. 1–31, 2022.

[18] W. Alam, A. Mehmood, K. Ali, U. Javaid, S. Alharbi, and J. Iqbal, "Nonlinear control of a flexible joint robotic manipulator with experimental validation," *Strojniški vestnik - Journal of Mechanical Engineering*, vol. 64, no. 1, jan 2018.

[19] O. M. Omisore, S. Han, J. Xiong, H. Li, Z. Li, and L. Wang, "A review on flexible robotic systems for minimally invasive surgery," *IEEE Transactions on Systems, Man, and Cybernetics: Systems*, vol. 52, no. 1, pp. 631–644, jan 2022.

[20] F. Guo, T. Sun, P. Wang, S. Liu, B. Lian, and Y. Song, "Multi-stability of a planar three-limb flexible mechanism," *Mechanism and Machine Theory*, vol. 175, p. 104956, sep 2022.

[21] J. Meijaard and V. van der Wijk, "Dynamic balancing of mechanisms with flexible links," *Mechanism and Machine Theory*, vol. 172, p. 104784, jun 2022.

[22] S. S. Lone, N. Z. Azlan, and N. Kamarudzaman, "Soft pneumatic exoskeleton for wrist and thumb rehabilitation," *International Journal of Robotics and Control Systems*, vol. 1, no. 4, pp. 440–452, oct 2021.

[23] M. Tahmasebi, M. Gohari, and A. Emami, "An autonomous pesticide sprayer robot with a color-based vision system," *International Journal of Robotics and Control Systems*, vol. 2, no. 1, pp. 115–123, feb 2022.

[24] Y. Lu, Z. Chang, Y. Lu, and Y. Wang, "Development and kinematics/statics analysis of rigid-flexible-soft hybrid finger mechanism with standard force sensor," *Robotics and Computer-Integrated Manufacturing*, vol. 67, p. 101978, feb 2021.

[25] Y. Feng, Z. Ji, Y. Gao, H. Zheng, and J. Tan, "An energy-saving optimization method for cyclic pick-and-place tasks based on flexible joint configurations," *Robotics and Computer-Integrated Manufacturing*, vol. 67, p. 102037, feb 2021.

[26] A.-N. Sharkawy, "Effect of joints' configuration change on the effective mass of the robot," *International Journal of Robotics and Control Systems*, vol. 2, no. 1, pp. 105–114, feb 2022.

[27] S. Yi and J. Zhai, "Adaptive second-order fast nonsingular terminal sliding mode control for robotic manipulators," *ISA Transactions*, vol. 90, pp. 41–51, jul 2019.

[28] J. Park and Y. Choi, "Input-to-state stability of variable impedance control for robotic manipulator," *Applied Sciences*, vol. 10, no. 4, p. 1271, feb 2020.

[29] D. Chen, S. Li, Q. Wu, and X. Luo, "Super-twisting ZNN for coordinated motion control of multiple robot manipulators with external disturbances suppression," *Neurocomputing*, vol. 371, pp. 78–90, jan 2020.

[30] Y. Kali, M. Saad, and K. Benjelloun, "Optimal super-twisting algorithm with time delay estimation for robot manipulators based on feedback linearization," *Robotics and Autonomous Systems*, vol. 108, pp. 87–99, oct 2018.

[31] ——, "Control of robot manipulators using modified backstepping sliding mode," in *New Developments and Advances in Robot Control*. Springer Singapore, 2019, pp. 107–136.

[32] V. T. Yen, W. Y. Nan, and P. V. Cuong, "Recurrent fuzzy wavelet neural networks based on robust adaptive sliding mode control for industrial robot manipulators," *Neural Computing and Applications*, vol. 31, no. 11, pp. 6945–6958, may 2018.

[33] S. Zaare, M. R. Soltanpour, and M. Moattari, "Voltage based sliding mode control of flexible joint robot manipulators in presence of uncertainties," *Robotics and Autonomous Systems*, vol. 118, pp. 204–219, aug 2019.

[34] F. Campisano, S. Caló, A. A. Remirez, J. H. Chandler, K. L. Obstein, R. J. Webster, and P. Valdastri, "Closed-loop control of soft continuum manipulators under tip follower actuation," *The International Journal of Robotics Research*, vol. 40, no. 6-7, pp. 923–938, mar 2021.

[35] A. J. Abougarair, M. K. I. Aburakhis, and M. M. Edardar, "Adaptive neural networks based robust output feedback controllers for nonlinear systems," *International Journal of Robotics and Control Systems*, vol. 2, no. 1, pp. 37–56, jan 2022.

[36] S. A. Ajwad, J. Iqbal, R. U. Islam, A. Alsheikhy, A. Almeshal, and A. Mehmood, "Optimal and robust control of multi DOF robotic manipulator: Design and hardware realization," *Cybernetics and Systems*, vol. 49, no. 1, pp. 77–93, jan 2018.

[37] M. Van, X. P. Do, and M. Mavrovouniotis, "Self-tuning fuzzy PID-nonsingular fast terminal sliding mode control for robust fault tolerant control of robot manipulators," *ISA Transactions*, vol. 96, pp. 60–68, jan 2020.

[38] K. Khnissi, C. B. Jabeur, and H. Seddik, "A smart mobile robot commands predictor using recursive neural network," *Robotics and Autonomous Systems*, vol. 131, p. 103593, sep 2020.

[39] X. Liu, C. Yang, Z. Chen, M. Wang, and C.-Y. Su, "Neuro-adaptive observer based control of flexible joint robot," *Neurocomputing*, vol. 275, pp. 73–82, jan 2018.

[40] T. Rybus, K. Seweryn, and J. Z. Sasiadek, "Nonlinear model predictive control (NMPC) for free-floating space manipulator," in *GeoPlanet: Earth and Planetary Sciences*. Springer International Publishing, nov 2018, pp. 17–29.

[41] C. Yang, G. Peng, L. Cheng, J. Na, and Z. Li, "Force sensorless admittance control for teleoperation of uncertain robot manipulator using neural networks," *IEEE Transactions on Systems, Man, and Cybernetics: Systems*, pp. 1–11, 2019.

[42] M. R. Soltanpour, S. Zaare, M. Haghgoo, and M. Moattari, "Free-chattering fuzzy sliding mode control of robot manipulators with joints flexibility in presence of matched and mismatched uncertainties in model dynamic and actuators," *Journal of Intelligent & Robotic Systems*, apr 2020.

[43] T. V. Nguyen, N. H. Thai, H. T. Pham, T. A. Phan, L. Nguyen, H. X. Le, and H. D. Nguyen, "Adaptive neural network-based backstepping sliding mode control approach for dual-arm robots," *Journal of Control, Automation and Electrical Systems*, vol. 30, no. 4, pp. 512–521, may 2019.

[44] R. Fareh, M. R. Saad, M. Saad, A. Brahmi, and M. Bettayeb, "Trajectory tracking and stability analysis for mobile manipulators based on decentralized control," *Robotica*, vol. 37, no. 10, pp. 1732–1749, mar 2019.

[45] H. Khajehsaeid, B. Esmaeili, R. Soleymani, and A. Delkhosh, "Adaptive back stepping fast terminal sliding mode control of robot manipulators actuated by pneumatic artificial muscles: continuum modelling, dynamic formulation and controller design," *Meccanica*, vol. 54, no. 8, pp. 1203–1217, jun 2019.

[46] A. J. Muñoz-Vázquez, F. Gaxiola, F. Martínez-Reyes, and A. Manzo-Martínez, "A fuzzy fractional-order control of robotic manipulators with PID error manifolds," *Applied Soft Computing*, vol. 83, p. 105646, oct 2019.

[47] A. H. Khan, S. Li, and X. Luo, "Obstacle avoidance and tracking control of redundant robotic manipulator: An RNN-based metaheuristic approach," *IEEE Transactions on Industrial Informatics*, vol. 16, no. 7, pp. 4670–4680, jul 2020.

[48] S. Zaare and M. R. Soltanpour, "Continuous fuzzy nonsingular terminal sliding mode control of flexible joints robot manipulators based on nonlinear finite time observer in the presence of matched and mismatched uncertainties," *Journal of the Franklin Institute*, vol. 357, no. 11, pp. 6539–6570, jul 2020.

[49] N. M. H. Norsahperi and K. A. Danapalasingam, "A comparative study of LQR and integral sliding mode control strategies for position tracking control of robotic manipulators," *International journal of electrical and computer engineering systems*, vol. 10, no. 2, pp. 73–83, jan 2020.

[50] R. Colombo, F. Gennari, V. Annem, P. Rajendran, S. Thakar, L. Bascetta, and S. K. Gupta, "Parameterized model predictive control of a nonholonomic mobile manipulator: A terminal constraint-free approach," in *IEEE 15th International Conference on Automation Science and Engineering (CASE)*. IEEE, aug 2019.

[51] M. Esfandiari, S. Chan, G. Sutherland, and D. Westwick, "Nonlinear model predictive control of robot manipulators using quasi-LPV representation," in *7th International Conference on Control, Mechatronics and Automation (ICCMA)*. IEEE, nov 2019.

[52] M. M. Morato, J. E. Normey-Rico, and O. Sename, "Model predictive control design for linear parameter varying systems: A survey," *Annual Reviews in Control*, vol. 49, pp. 64–80, 2020.

[53] Y. A. Younes and M. Barczyk, "A backstepping approach to nonlinear model predictive horizon for optimal trajectory planning," *Robotics*, vol. 11, no. 5, p. 87, aug 2022.

[54] S. Kandasamy, M. Teo, N. Ravichandran, A. McDaid, K. Jayaraman, and K. Aw, "Body-powered and portable soft hydraulic actuators as prosthetic hands," *Robotics*, vol. 11, no. 4, p. 71, jul 2022.

[55] C. A. P. Fernndez, "Stabilizing model predictive control for wheeled mobile robots with linear parameter-varying and different time-scales," in *Latin American Robotic Symposium, 2018 Brazilian Symposium on Robotics (SBR) and 2018 Workshop on Robotics in Education (WRE)*. IEEE, nov 2018.

[56] J. L. T. Besselmann and M. Morari, "Explicit mpc for lpv systems: Stability and optimality," *IEEE Transactions on Automatic Control*, vol. 57, no. 9, pp. 2322–2332, 2012.

[57] Y. Yang, T. Dai, C. Hua, and J. Li, "Composite NNs learning full-state tracking control for robotic manipulator with joints flexibility," *Neurocomputing*, vol. 409, pp. 296–305, oct 2020.

[58] M. H. Korayem, N. Ghobadi, and S. F. Dehkordi, "Designing an optimal control strategy for a mobile manipulator and its application by considering the effect of uncertainties and wheel slipping," *Optimal Control Applications and Methods*, vol. 42, no. 5, pp. 1487–1511, may 2021.

[59] Y. Zhang, S. Li, J. Zou, and A. H. Khan, "A passivity-based approach for kinematic control of manipulators with constraints," *IEEE Transactions on Industrial Informatics*, vol. 16, no. 5, pp. 3029–3038, may 2020.

[60] X. Gao, L. Yan, and C. Gerada, "Modeling and analysis in trajectory tracking control for wheeled mobile robots with wheel skidding and slipping: Disturbance rejection perspective," *Actuators*, vol. 10, no. 9, p. 222, sep 2021.

[61] C. A. P. Fernández, "Oriented manifold-based error tracking control for nonholonomic wheeled autonomous vehicles on lie group for curvilinear approach," *Latin American Journal of Development*, vol. 3, no. 6, pp. 3608–3626, nov 2021.

[62] S. Liu, K. Liu, Z. Zhong, J. Yi, and H. Aliev, "A novel wheeled mobile robots control based on robust hybrid controller: Mixed h2/h∞ and predictive algorithm approach," *Journal of King Saud University - Computer and Information Sciences*, dec 2021.

[63] P. Righettini, R. Strada, and F. Cortinovis, "Modal kinematic analysis of a parallel kinematic robot with low-stiffness transmissions," *Robotics*, vol. 10, no. 4, p. 132, dec 2021.

[64] D. Subedi, I. Tyapin, and G. Hovland, "Dynamic modeling of planar multi-link flexible manipulators," *Robotics*, vol. 10, no. 2, p. 70, may 2021.

[65] C. Holmes, "Practical design considerations for performance and robustness in the face of uncertain flexible dynamics in space manipulators," *Frontiers in Robotics and AI*, vol. 8, sep 2021.

[66] T. Kato, "Nonstationary flows of viscous and ideal fluids in r3," *Journal of Functional Analysis*, vol. 9, no. 3, pp. 296–305, mar 1972.

[67] K. M. Lynch and F. C. Park, *Modern Robotics: Mechanics, Planning, and Control*, C. U. P. (1st ed.), Ed., 2017.

[68] X. Ma, Y. Zhao, and Y. Di, "Trajectory tracking control of robot manipulators based on u-model," *Mathematical Problems in Engineering*, vol. 2020, pp. 1–10, may 2020.

[69] V. Powers and B. Reznick, "A new bound for pólya's theorem with applications to polynomials positive on polyhedra," *Journal of Pure and Applied Algebra*, vol. 164, no. 1-2, pp. 221–229, 2001.